Active DC-Bias Mitigation Method for a Single-Phase Transformer-Connected Converter through DC-Link Measurement

Active DC-bias mitigation method for a single-phase transformer-connected converter through DC-link measurement

Kaveh Pouresmaeil, Maurice Roes, Nico Baars, and Korneel Wijnands
Electromechanics and Power Electronics (EPE) group
Department of Electrical Engineering
Eindhoven University of Technology, the Netherlands
Email: k.pouresmaeil@tue.nl

***Abstract*—DC-bias in the magnetic flux is a common challenge for transformer-connected converters. Typically, in isolated switched-mode converters, it is induced by a DC current flowing through one or more windings of the transformer. This bias can increase the core losses of the transformer and drive the transformer core into saturation, which deteriorates the performance of the transformer and can even result in the malfunctioning of the converter. Conventional methods for DC-bias mitigation involve expensive sensing circuitry and/or impair the performance of the converter. The proposed method utilizes the fact the DC-bias current through the transformer will result in a switching-frequency current component in the DC-link current of the converter. A band-pass filter can for example be used to indirectly measure the switching-frequency current component and then mitigate that in a closed-loop manner. Both simulation results and experimental measurements are provided to verify the theoretical analysis and effectiveness of the proposed method.**

***Index Terms*—flux balancing, DC-bias, magnetic saturation, isolated converters, dual-active bridge**

I. INTRODUCTION

A wide range of power electronic applications requires galvanic isolation for the purpose of human safety and noise immunity. Transformers, which can transfer energy through a magnetic field, as opposed to direct electrical contact, are the main tool to provide the required isolation in power converters [1]. For a magnetic component to operate properly, it must work in its linear operating region. A transformer is usually designed so that under normal operation, i.e. when the excitation voltages are on average zero, it operates in this linear region. If, for any mismatch in circuit parameters or modulation waveforms, a transformer winding is subjected to a DC voltage, a DC-bias current flows through the windings, thereby taking the magnetic core outside its linear region. As a result, the magnetic core losses increase, leading to a higher energy consumption and heating of the transformer, or in worst case saturation can occur in the core, which leads to malfunctioning or even destruction of the power converter containing the transformer [2], [3].

Fig. 1 shows a transformer-connected single-phase DC/AC converter and its AC-link voltage. This converter is the building block of a large variety of isolated power electronic converters. For example, a dual active bridge converter can be formed by adding an active bridge and a DC-link to the secondary side of the transformer. In such a transformer-connected converter, volt-second imbalances are likely to occur on both sides of the transformer. To prevent biasing of the flux density in the transformer core, volt-second balancing of both the primary and secondary terminals of the transformer is demanded. Several active and passive methods have been proposed to mitigate the DC-bias current [4]. Active approaches generally detect the DC-bias current using transformer related variables, such as the magnetic flux and the winding current and voltage. This, however, requires expensive and high accuracy sensing circuitry [5]. Passive methods are also used to avoid transformer saturation, such as the introduction of DC-blocking capacitors in series with the transformer windings, inclusion of an air gap in the transformer core, and over dimensioning the flux density in the magnetic core, which can result in additional volume and/or power losses [6]. An alternative can be measuring quantities which are not directly

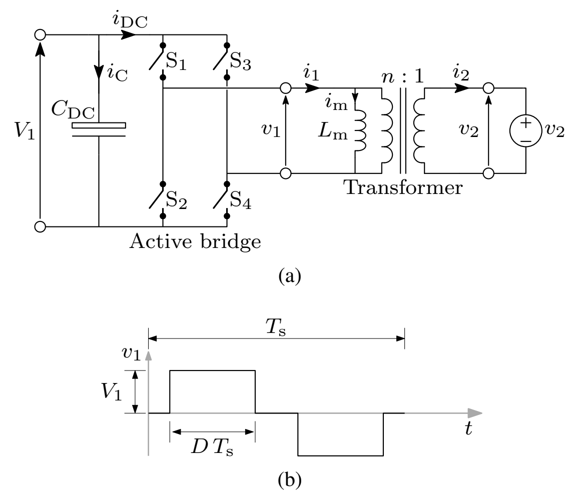

Fig. 1: (a) Typical transformer-connected DC/AC converter and (b) its AC-link voltage, whose duty cycle is represented by D.

related to the transformer.

If a DC-bias current exists in the AC-link of the converter, it will be unfolded by the bridge and then appear in the DC-link current as a switching-frequency component. The switched-mode operation of the bridge implies that the AC-side current appears alternately as a positive and negative current in the DC-link current. It can therefore be described as multiplication of the AC-side current by a pulse wave at the switching frequency. With this knowledge, this paper proposes a new method to detect the DC-bias in the magnetic flux by means of the indirect measurement of the switching-frequency component of the DC-link current, instead of measuring any quantity directly related to the transformer voltage or current. Theoretical analysis is conducted to establish the feasibility of the proposed DC-bias mitigation method. Simulation results and experimental measurements are provided to validate the theoretical analysis and practical feasibility of the proposed method.

II. DC-bias Mitigation

A. DC-bias detection

Volt-second imbalances are likely to be applied on both sides of the transformer shown in Fig. 1. To prevent DC-biasing of the flux density in the transformer core, volt-second balancing of both the primary and secondary terminals of the transformer is required. For simplicity, but without loss of generality, it is assumed that the voltage of the secondary side is free of a DC component, and it can be modeled as a voltage source. If the voltage waveform that the primary bridge applies to the transformer winding has a DC component, a DC-bias current will flow through the transformer in steady state operation.

The rectification of the converter, modeled as multiplication of the AC-side current by a square wave function $r(t)$, corresponds to a convolution operation in the frequency domain. Let $i_1(t)$ and $i_{\mathrm{DC}}(t)$ be the input and output signals of the rectifier. Then the DC-link current spectrum is given by [7]

$$i_{\mathrm{DC}}(t) = i_1(t)r(t) \leftrightarrow I_{\mathrm{DC}}(f) = I_1(f) * R(f) \tag{1}$$

The pulse wave, with a frequency equal to the switching frequency f_{s} and a duty cycle of D, can be represented by the following equation in the frequency domain [8]

$$R(f) \triangleq \sum_{k=0}^{\infty} \frac{4\sin((2k+1)\pi D)}{(2k+1)\pi}\delta(f-(2k+1)f_s), \tag{2}$$

If $i_1(t)$ happens to have a DC component, according to (1), $I_{\mathrm{DC}}(f)$ can be represented as

$$\begin{aligned}
I_{\mathrm{DC}}(f) &\triangleq \int_{-\infty}^{\infty} I_1(p)R(f-p)dp \\
&\triangleq \int_{-\infty}^{\infty}\left(\sum_{h=1}^{\infty} I_{1,h}(p) + I_{1,0}(p)\right)R(f-p)dp \\
&\triangleq \overbrace{\int_{-\infty}^{\infty}\sum_{h=1}^{\infty} I_{1,h}(p)R(f-p)dp}^{I_{\mathrm{DC,normal}}(f)} + \int_{-\infty}^{\infty} I_{1,0}(p)R(f-p)dp \\
&\triangleq I_{\mathrm{DC,normal}} + \int_{-\infty}^{\infty} I_{1,0}\delta(p)\times \\
&\qquad \sum_{k=0}^{\infty}\frac{4\sin((2k+1)\pi D)}{(2k+1)\pi}\delta(f-p-(2k+1)f_s)dp \\
&\triangleq I_{\mathrm{DC,normal}} + \sum_{k=0}^{\infty}\frac{4\sin((2k+1)\pi D)I_{1,0}}{(2k+1)\pi}\times \\
&\qquad \int_{-\infty}^{\infty}\delta(p)\delta(f-p-(2k+1)f_s)dp \\
&\triangleq I_{\mathrm{DC,normal}} + \\
&\qquad \sum_{k=0}^{\infty}\frac{4\sin((2k+1)\pi D)I_{1,0}}{(2k+1)\pi}\delta(f-(2k+1)f_s)
\end{aligned} \tag{3}$$

and will feature the switching-frequency component and its odd-order harmonics. In addition to the switching-frequency component and its harmonics in i_1, $I_{\mathrm{DC}}(f)$ will also have even-order harmonics represented by $I_{\mathrm{DC,normal}}$ in (3). Consequently, a switching-frequency component in the DC-link current indicates a DC-bias current through the transformer. By means of filtering and/or signal processing, this component can be detected, and then used to detect the DC-bias current. Possibly the simplest method is by diverting the switching-frequency harmonics component to a shunt path in the DC-link. This path should present a low-impedance path for the harmonic current component. Such as path is naturally provided by the DC-link capacitor. The voltage ripple of the DC-link capacitor can then be measured to detect the DC-bias. However, due to large DC and second-order harmonic components in the DC-link capacitor voltage, extraction of the switching-frequency component is not straightforward.

As show in Fig. 2, additional circuitry can be used in the DC-link to (partially) divert the switching-frequency component of the DC-link current $i_{\mathrm{DC},1}$ and then detect the DC-bias current. This additional circuitry can be either a band-pass filter or a high-pass filter, depending on whether the second-order harmonic component is desired to be attenuated. In this paper, a band-pass filter is used, to extract the switching-frequency current component. To this end, a series resonant LC filter that is tuned to the switching frequency of the bridge is placed in parallel with the DC-link capacitor C_{DC} to detect the switching-frequency-harmonic component $i_{\mathrm{DC},1}$ as shown in Fig. 3(a). Fig. 3(b) depicts a simplified representation of the converter to analyze DC-biased operation. The DC-link

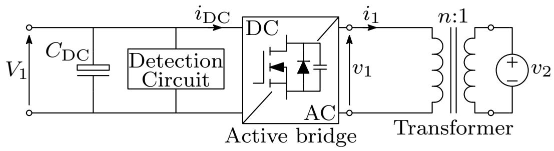

Fig. 2: Proposed detection scheme

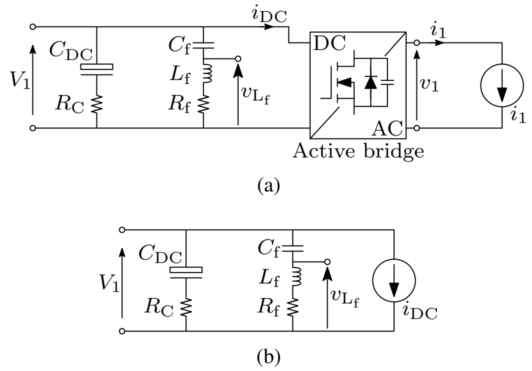

Fig. 3: (a) AC/DC converter with an LC band-pass filter in the DC-link and (b) simplified representation of it.

TABLE I: Circuit specifications

Description	Parameter	Value
Switching frequency	f_{s}	5 kHz
DC-link capacitance	C_{DC}	1 mF
DC-link resistance	R_{C}	0.15 Ω
Filter inductance	L_{f}	2.3 mH
Filter capacitance	C_{f}	470 nF
Filter resistance	R_{f}	0.7 Ω
Resonance frequency	f_{r}	4.84 kHz

terminals tend to present a high impedance at the switching frequency with respect to the DC-link capacitance, and are therefore modeled as an open connection. The voltage $v_{\mathrm{L_f}}$ is the measured variable to detect the DC-bias current. The transfer function of the DC-link current to the filter inductor voltage can written as

$$G(s) = \frac{V_{\mathrm{L_f}}}{I_{\mathrm{DC}}} = -\frac{R_{\mathrm{C}} L_{\mathrm{f}} s^2 + (\frac{L_{\mathrm{f}}}{C_{\mathrm{DC}}} + R_{\mathrm{C}} R_{\mathrm{f}})s + \frac{R_f}{C_{\mathrm{DC}}}}{L_{\mathrm{f}} s^2 + (R_{\mathrm{C}} + R_{\mathrm{f}})s + \frac{1}{C_{\mathrm{DC}}} + \frac{1}{C_{\mathrm{f}}}}, \quad (4)$$

where L_{f}, C_{DC} and C_{f} represent the inductance and capacitance of the band-pass filter and the DC-link capacitance of the converter, respectively. Additionally, R_{C} and R_{f} are the respective resistances for the DC-link capacitor and inductor used in the band-pass filter. Fig. 4 shows the bode diagram of $G(s)$ for the circuit parameters that are provided in Tab. I. As can be seen, by setting the resonance frequency a bit lower than the switching frequency, the voltage $v_{\mathrm{L_f}}(t)$ that appears across the filter inductor will have a phase shift of almost $180°$ with regard to $i_{\mathrm{DC},1}$ and the phase of $G(s)$ is has a low sensitivity to frequency variation.

As shown in Fig. 1, the active bridge is realized as a full-bridge that switches with a duty cycle of D. Hence, in steady-

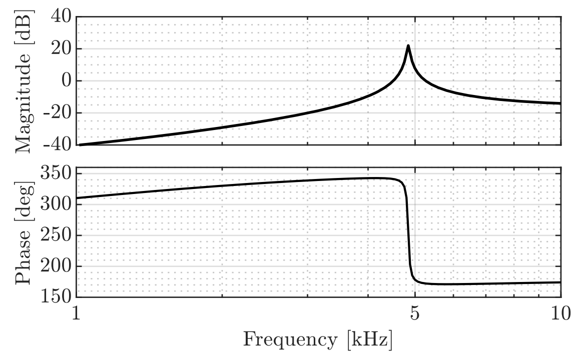

Fig. 4: Bode diagram of the transfer function of the DC-link current to the filter inductor voltage.

state, the switching-frequency harmonic of the bridge current $i_{\mathrm{DC},1}$ follows from

$$i_{\mathrm{DC},1} = \frac{4I_{1,0}}{\pi}\sin(\pi D)\sin(\omega_{\mathrm{s}} t), \quad (5)$$

where $I_{1,0}$ and ω_{s} represent the amplitude of the DC component of i_1 and the angular switching frequency of the full-bridge, respectively. In addition to the first-order harmonic component and the other odd-order components, resulting from the DC-bias current, the filter inductor voltage inherently contains even-order harmonic components, of which the second-order one is predominant. As a result, the filter inductor voltage can be written as

$$v_{\mathrm{L_f}}(t) = (\hat{V}_{\mathrm{L_f}})_1 \sin(\omega_{\mathrm{s}} t + \varphi_1) + \sum_{h=2}^{\infty} (\hat{V}_{\mathrm{L_f}})_h \sin(h\omega_{\mathrm{s}} t + \varphi_h), \quad (6)$$

Although the even-order components are attenuated by the band-pass filter, they can be a source of error when the filter inductor voltage is fed into a feedback loop for control of the transformer bias current. On the other hand, the odd-order components results from the DC-bias current through the transformer. Since the undesired harmonics in the filter inductor voltage are of even order, they can be mitigated by sampling at the right moment. Fig. 6 depicts the typical waveform for the filter inductor voltage under a positive DC-bias current through the transformer. The inductor voltage can be sampled twice within each switching cycle upon a Start of Conversion Signal (SOC). SOC1 and SOC2 are aligned with $t = \frac{T_{\mathrm{s}}}{4}$ and $t = \frac{3T_{\mathrm{s}}}{4}$ in each switching cycle, respectively. By subtracting two consecutive samples of the inductor voltage upon SOC2,

$$\begin{aligned} v_{\mathrm{fd}}[n] &= v_{\mathrm{L_f}}[n] - v_{\mathrm{L_f}}[n-1] \\ &= v_{\mathrm{L_f}}(t = \frac{3T_{\mathrm{s}}}{4}) - v_{\mathrm{L_f}}(t = \frac{T_{\mathrm{s}}}{4}) \\ &= -2\sum_{h=0}^{\infty} (\hat{V}_{\mathrm{L_f}})_{2h+1} \cos(\varphi_{2h+1}), \end{aligned} \quad (7)$$

the effect of even harmonics is mitigated. Here, the remaining term is proportional to the DC-bias current through the trans-

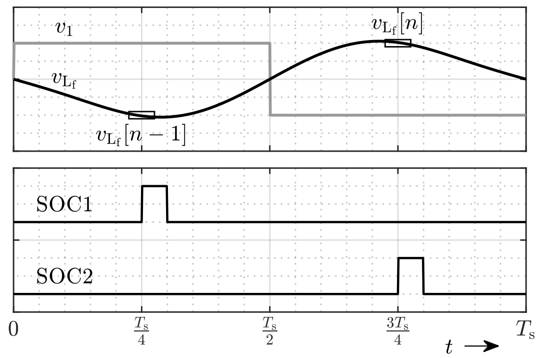

Fig. 5: Waveforms of the bridge AC voltage v_1, filter inductor voltage $v_{\mathrm{L_f}}$ and SOCs.

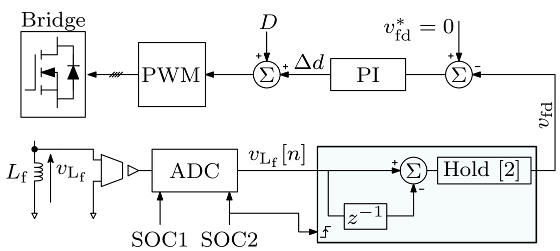

Fig. 6: Control scheme for the proposed method.

former. Hence, $v_{\mathrm{fd}}[n]$ is fed into the feedback loop to actively compensate the DC-bias current.

B. Closed loop control

Fig. 6 represents the developed control scheme to mitigate the DC-bias current through the transformer. The filter inductor voltage $v_{\mathrm{L_f}}$ is sampled at the middle of the positive and negative half-cycles of the bridge voltage v_1. The sampled values of these instances are subtracted upon acquisition of the second sample, and the derived value is held until the next subtraction operation. The resulting variable v_{fd}, which is linearly related to the DC-bias current, is compared with the set point and fed into a PI controller. The output of this controller is the modification (Δd) in the duty cycle of the PWM modulator to mitigate the DC voltage component in the bridge voltage.

III. Simulation Results

To verify the theoretical analysis, simulations were conducted using PLECS with the circuit parameters given in Tab. I and $L_{\mathrm{m}} = 20\,\mathrm{mH}$ and $V_1 = 400\,\mathrm{V}$. In Fig. 7, the behavior of the magnetizing current i_{m} and filter inductor voltage $v_{\mathrm{L_f}}$ are shown before and after enabling the closed-loop DC-bias control. A timing mismatch ($t = 20\,\mathrm{ns}$) was implemented in the PWM modulator of the converter, which means that the positive half-cycle of v_1 is extended by the timing mismatch, and as can be seen in Fig. 7(b), the magnetizing current presents a positive DC component before enabling the closed-loop control. The controller is enabled at $t = 20\,\mathrm{ms}$ and

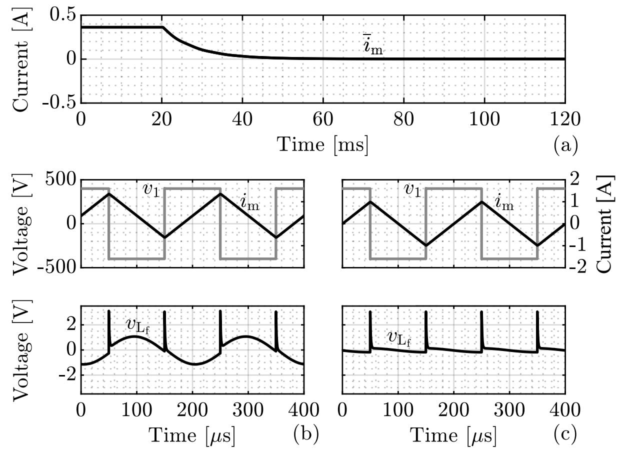

Fig. 7: Simulated behavior of the closed-loop system: (a) average magnetizing current $\bar{i}_{\mathrm{m}}$, winding voltage v_1, magnetizing current i_{m}, and filter inductor voltage $v_{\mathrm{L_f}}$ (b) before and (c) after enabling the closed-loop controller.

successfully mitigates the DC-bias current through the transformer, as can be seen from the average magnetizing current $\bar{i}_{\mathrm{m}}$ in Fig. 7(a), and the steady state current i_{m} in Fig. 7(b) and Fig. 7(c).

IV. Experimental Verification

To validate the theoretical analysis and effectiveness of the proposed method, experimental measurements are conducted on a transformer-connected converter prototype. Each phase leg consists of two SIC MOSFETs (NTHL020N120SC1) [9]. The converter is connected to the primary winding of a transformer with unity turn-ratio and a magnetizing inductance $L_{\mathrm{m}} = 20\,\mathrm{mH}$. The secondary winding is connected to an RL load ($R_{\mathrm{L}} = 14.7\,\Omega$ and $L_{\mathrm{L}} = 295\,\mu\mathrm{H}$). The other parameters are provided in Tab. I. Fig. 8 illustrates the behavior of the primary winding current and the filter inductor voltage when the closed-loop DC-bias control is activated. Given the large resistance of the load compared to that of the DC current path, the DC component of the primary winding current $\bar{i}_1$ exhibits similar magnitudes and dynamic behavior to the average magnetizing current $\bar{i}_{\mathrm{m}}$. A timing mismatch of $300\,\mathrm{ns}$ has been introduced to the converter, resulting in a positive DC component in the primary winding current i_1 before the closed-loop control is enabled. The controller is enabled at $t = 20\,\mathrm{ms}$ and successfully mitigates the DC-bias current through the transformer, as can be seen in Fig. 8(b) and Fig. 8(c).

V. Conclusions

A new DC-bias current mitigation method has been proposed for transformer-connected converters in this paper. It has been found that the DC-bias current in the AC-link of the converter is unfolded by the bridge and then appears in the DC-link current as a switching-frequency component. Detecting this switching frequency component is straightforward, and can be for example achieved using a band-pass filter that

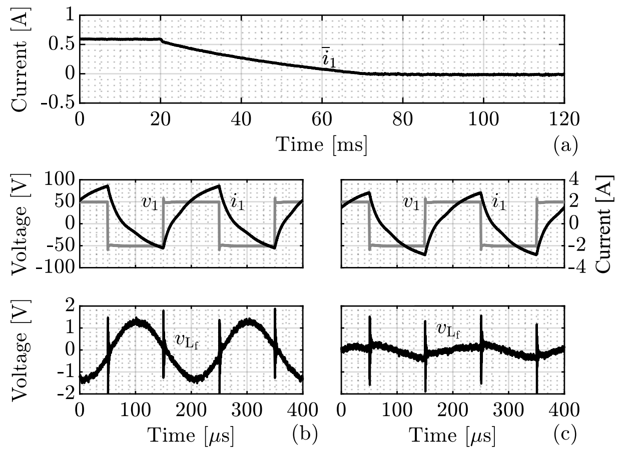

Fig. 8: Experimental measurement for the closed-loop system: (a) average primary winding current $\bar{i}_1$, primary winding voltage v_1, primary winding current i_1, the filter inductor voltage $v_{\mathrm{L_f}}$ (b) before and (c) after enabling the closed-loop controller.

is tuned to the switching frequency and placed in the DC-link of the converter. It has be shown that by sampling the filter inductor voltage at twice the switching frequency and subtracting the consecutive samples, the remaining term is linearly proportional to the DC-bias current through the transformer. Using this term as the feedback variable, a closed-loop control scheme has been developed to regulate the DC-bias current to zero. The closed-loop system has been verified through both simulation results and experimental measurements. The proposed scheme can be implemented in a wide range of transformer-connected converters to detect and mitigate the DC-bias current through the transformer without requiring expensive measurement circuitry nor impairing the performance of the converter.

ACKNOWLEDGMENT

This publication is part of the project NEON (with project number 17628 of the research programme Crossover which is (partly) financed by the Dutch Research Council (NWO)).

REFERENCES

[1] N. M. L. Tan, T. Abe and H. Akagi, "Topology and application of bidirectional isolated DC-DC converters," 8th International Conference on Power Electronics - ECCE Asia, Jeju, Korea (South), 2011, pp. 1039-1046, doi: 10.1109/ICPE.2011.5944690.

[2] Z. Wang, C. Li, J. Liu and Z. Zheng, "DC Bias Elimination and Soft Switching in Transient State of Dual-Active-Bridge DC-DC Converter," IECON 2022 – 48th Annual Conference of the IEEE Industrial Electronics Society, Brussels, Belgium, 2022, pp. 1-6, doi: 10.1109/IECON49645.2022.9968411.

[3] S. Xu, D. Chen and H. Zeng, "A Magnetic Saturation Suppression Scheme of The Output Line-Frequency Transformer in Photovoltaic Inverter," IECON 2020 The 46th Annual Conference of the IEEE Industrial Electronics Society, Singapore, 2020, pp. 3643-3647, doi: 10.1109/IECON43393.2020.9254358.

[4] G. Ortiz, J. Mühlethaler and J. W. Kolar, ""Magnetic Ear"-based balancing of magnetic flux in high power medium frequency dual active bridge converter transformer cores," 8th International Conference on Power Electronics - ECCE Asia, Jeju, Korea (South), 2011, pp. 1307-1314, doi: 10.1109/ICPE.2011.5944377.

[5] J. Voss, S. P. Engel and R. W. De Doncker, "Control Method for Avoiding Transformer Saturation in High-Power Three-Phase Dual-Active Bridge DC–DC Converters," in IEEE Transactions on Power Electronics, vol. 35, no. 4, pp. 4332-4341, April 2020, doi: 10.1109/TPEL.2019.2938585.

[6] S. A. Assadi, H. Matsumoto, M. Moshirvaziri, M. Nasr, M. S. Zaman and O. Trescases, "Active Saturation Mitigation in High-Density Dual-Active-Bridge DC–DC Converter for On-Board EV Charger Applications," in IEEE Transactions on Power Electronics, vol. 35, no. 4, pp. 4376-4387, April 2020, doi: 10.1109/TPEL.2019.2939301.

[7] A. V. Oppenheim, A. S. Willsky, and S. H. Nawab. 1996. "Signals and systems (2nd ed.)." Prentice-Hall, Inc., USA.

[8] C. Hurley and J. McLean. "Wavelet: Analysis and Methods." 2018. EDTECH, United Kingdom.

[9] Imperix, "Half-bridge SiC power module," PEB8038 datasheet, [Revised Feb. 2023].